- The land sink anomaly of 2011 was very short-lived in semi-arid Australia
- An *Acacia* woodland returned to carbon neutrality post-2011
- An open *Corymbia* savanna was a very large carbon source post-2011
- Access to groundwater by *Corymbia* in the savanna was inferred from leaf ^{13}C
- Groundwater contributed to evapotranspiration excess in a year of average rainfall

1 **Productivity and evapotranspiration of two contrasting semiarid ecosystems**
2 **following the 2011 carbon land sink anomaly**

3 James CLEVERLY*[a,b], Derek EAMUS[a,b], Eva VAN GORSEL[c], Chao CHEN[a,1], Rizwana
4 RUMMAN[a], Qunying LUO[d], Natalia RESTREPO COUPE[d], Longhui LI[a], Natascha
5 KLJUN[e], Ralph FAUX[a], Qiang YU[a] and Alfredo HUETE[d]

6 [a] School of Life Sciences, University of Technology Sydney, PO Box 123, Broadway,
7 NSW, 2007, Australia

8 [b] Australian Supersite Network, Terrestrial Ecosystem Research Network, University of
9 Technology Sydney, PO Box 123, Broadway, NSW, 2007, Australia

10 [c] CSIRO Marine and Atmospheric Research, Pye Laboratory, Clunies Ross Street, Acton,
11 ACT 2600, Australia

12 [d] Climate Change Cluster, University of Technology Sydney, PO Box 123, Broadway,
13 NSW, 2007, Australia

14 [e] Department of Geography, Swansea University, Singleton Park, Swansea SA2 8PP, UK

15 *Correspondence: James.Cleverly@UTS.edu.au, +61 (02) 9514 8405, +61 (02) 9514
16 4079 (FAX)

17 **Keywords:** *Corymbia* **savanna;** *Acacia* **woodland; evapotranspiration; net**
18 **ecosystem productivity; water-use efficiency; global 2011 land**
19 **sink anomaly**
20

1

[1] Present address: CSIRO Agriculture Flagship, PMB 5, PO Wembley, WA, 6913, Australia

21   **ABSTRACT**

22   Global carbon balances are increasingly affected by large fluctuations in

23   productivity occurring throughout the semiarid regions. Recent analyses found a large C

24   uptake anomaly in 2011 in arid and semiarid regions of the southern hemisphere.

25   Consequently, we compared the C and water fluxes of two distinct woody ecosystems (a

26   Mulga (*Acacia*) woodland and a *Corymbia* savanna) between August 2012 and August

27   2014 in semiarid central Australia, demonstrating that the 2011 anomaly was short-lived

28   in both ecosystems. The Mulga woodland was approximately C neutral but with periods

29   of significant uptake within both years. The extreme drought tolerance of *Acacia* is

30   presumed to have contributed to this. By contrast, the *Corymbia* savanna was a very large

31   net C source (130 and 200 g C m^{-2} yr^{-1} in average and below average rainfall years,

32   respectively), which is likely to have been a consequence of the degradation of standing,

33   senescent biomass that was a legacy of high productivity during the 2011 anomaly. The

34   magnitude and temporal patterns in ecosystem water-use efficiencies (WUE), derived

35   from eddy covariance data, differed across the two sites, reflecting differences in the

36   relative contributions of respiration to net C fluxes across the two ecosystems. In contrast,

37   differences in leaf-scale measures of WUE, derived from ^{13}C stable isotope analyses, were

38   apparent at small spatial scales and may reflect the different rooting strategies of

39   *Corymbia* and *Acacia* trees within the *Corymbia* savanna. Restrictions on root growth and

40   infiltration by a siliceous hardpan located below *Acacia*, whether in the Mulga woodland

41   or in the Mulga patches of the *Corymbia* savanna, impedes drainage of water to depth,

42   thereby producing a reservoir for soil moisture storage under *Acacia* while acting as a

43   barrier to access of groundwater by *Corymbia* trees in Mulga patches, but not in the open

44   *Corymbia* savanna.

45

1. Introduction

Inter-annual variability in atmospheric concentrations of CO_2 is large (Le Quéré et al., 2014), and much of this variability is driven by fluctuations in the source/sink strength of terrestrial ecosystems (Cox et al., 2013). During the latter half of the twentieth century, global net primary productivity (NPP) may have increased (Nemani et al., 2003), resulting in a potential increase in uptake of 0.05 Pg C per year (Ballantyne et al., 2012). Then, global NPP was reduced by 0.55 Pg C during the period 2000–2009, a result ascribed to large-scale drought in the southern hemisphere (Zhao and Running, 2010). Thereafter, Le Quéré et al. (2014) identified the 2011 land sink anomaly, which was a year of exceptional productivity, and Poulter et al. (2014) confirmed this anomaly by using a combination of modelling and remote sensing approaches. This land sink anomaly was driven by growth in semiarid vegetation of the southern hemisphere, with almost 60% occurring in Australia (Poulter et al., 2014). We have previously shown, using field observations of landscape fluxes of CO_2, that one of the dominant ecosystems of semiarid central Australia was indeed a large sink for C over almost all of the 12 months between October 2010 and October 2011 (Cleverly et al., 2013a; Eamus et al., 2013). Large fluctuations in productivity, evapotranspiration (ET) and ecosystem water-use efficiency (eWUE) across these semiarid regions reflect the very high ecosystem resilience of vegetation (Campos et al., 2013), which can have large effects on global C relations and consequently drive events such as the land sink anomaly of 2011.

Globally, dryland regions (arid, semiarid, and subhumid) cover 41% of the land area (Reynolds et al., 2007). Within these regions, arid and semiarid environments are characterised by chronic water shortages. Thus, productivity and ET are closely dependent upon the timing, frequency and amount of precipitation (Huxman et al., 2004), through which plant water availability is mediated by local hydrology (Breshears et al.,

3

71   2009; Loik et al., 2004; Reynolds et al., 2004). Terrain, soil texture, vegetation and

72   precipitation intensity influence runoff (Ludwig et al., 2005), while soil moisture

73   responses to precipitation pulses can depend upon runoff patterns, soil structure, rooting

74   dynamics, the spatial distribution of vegetation, and infiltration *versus* evaporation from

75   topsoil (Breshears et al., 2009; Ludwig et al., 2005; Martinez-Meza and Whitford, 1996).

76   Variation in local moisture availability is dependent upon rainfall pulses such that the

77   amount of precipitation required to induce a response in semiarid and arid vegetation is

78   dependent upon soil moisture storage capacity and run-off *versus* infiltration patterns

79   (Huxman et al., 2004; Ludwig et al., 2005; Ogle and Reynolds, 2004; Schwinning et al.,

80   2004). Together, these hydrologic factors influence the occurrence and timing of

81   respiratory pulses (one day following precipitation), pulses of productivity (3–4 days, if

82   present), and the exponential decline of ET following rainfall (Eamus et al., 2013;

83   Huxman et al., 2004). A detailed understanding of the variations in ecohydrology within

84   these regions is thus required to predict the source/sink strengths of water-limited

85   ecosystems.

86   The semiarid regions of Australia are dominated by three major biomes along a

87   woodland-savanna-grassland continuum: (1) Mulga woodlands (*Acacia* spp.), which

88   cover approximately 20–25% of the continental land area (Bowman et al., 2008), and (2)

89   *Corymbia* savanna over a hummock grass (*Triodia* spp.) understorey that grades into (3)

90   treeless hummock grasslands. Mulga trees range in height (2–10 m) and ground cover

91   (10–70%) (Nix and Austin, 1973), and they are preferentially located where storage of soil

92   moisture occurs near the surface in sand dunes, clay-rich soil or over the siliceous

93   hardpans that are common across semiarid Australia (Bowman et al., 2007; Ludwig et al.,

94   2005; Maslin and Reid, 2012; Nano and Clarke, 2010; Nix and Austin, 1973; Thiry et al.,

95   2006; Tongway and Ludwig, 1990). In contrast, tree density (stems per hectare) and cover

96 in *Corymbia* savannas are very low, and tree height ranges from 5–15 m. *Corymbia*

97 *opaca* is deep-rooted (8–20 m), and tends to be groundwater dependent in semiarid areas

98 (Cook and O'Grady, 2006; O'Grady et al., 2006a; O'Grady et al., 2006b). The understory

99 in the *Corymbia* savanna is characterised by a continuous cover of perennial hummock

100 grasses (*Triodia* spp.), which are widespread throughout Australia and cover an additional

101 20–25% of the continental land area (Bowman et al., 2008; Nano and Clarke, 2010; Reid

102 et al., 2008).

103   The aim of this study was to investigate fluctuations in the fluxes of C and water

104 from iconic Australian semiarid vegetation in response to reductions in precipitation

105 subsequent to the 2011 land sink anomaly. In this manuscript we compare and contrast

106 the behaviour of two disparate arid-zone tropical ecosystems (Mulga woodland and

107 *Corymbia* savanna) in central Australia to address four over-arching questions: (a) did the

108 2011 anomaly persist into 2012/2013/2014 in either biome; (b) do these two contrasting

109 ecosystems respond similarly to almost identical weather patterns; (c) how do ecosystem

110 water-use efficiencies compare across ecosystems; and (d) at small spatial scales within

111 the *Corymbia* savanna, how do leaf-scale water-use efficiencies across the two tree species

112 (*Acacia* and *Corymbia*) differ?

113

114 **2. Materials and Methods**

115 **2.1. Site descriptions**

116   This study was located on Pine Hill cattle station in the Ti Tree catchment of

117 central Australia and was co-located with several previous hydrological, ecological and

118 ecophysiological studies (Calf et al., 1991; Cleverly et al., 2013a; Eamus et al., 2013;

119 Harrington et al., 2002; Ma et al., 2013; O'Grady et al., 2009; Scanlon et al., 2006). The

120 Ti Tree catchment is an enclosed basin that covers 5,500 km^2 and contains two main

121 ecosystems: Mulga woodlands and *Corymbia* savanna (Harrington et al., 2002).

122 Measurements were collected from two locations: one in the Mulga woodland and one in

123 the *Corymbia* savanna. An eddy covariance tower was located in each ecosystem,

124 separated by 40 km at the same latitude ([22.3 °S 133.25 °E] and [22.3 °S 133.65 °E]).

125   A full description of the soil, floristics, leaf area index (LAI), energy balance and

126 C relations of the Mulga woodland can be found in Cleverly et al. (2013a) and Eamus et

127 al. (2013). Briefly, the Mulga woodland is characterised by a discontinuous canopy of

128 short (3–7 m), evergreen *Acacia* trees (*A. aptaneura* and *A. aneura*) with an understorey

129 of shrubs, herbs and grasses (C_3 and C_4) that are conditionally active depending upon

130 moisture availability and season (Cleverly et al., 2013a). The cover of *Acacia* is 74.5 % of

131 the land area in the Mulga woodland; *C. opaca* is essentially absent from the Mulga

132 woodland (one tree within the EC footprint, cf. Section 2.2). The basal area of *Acacia*

133 within the woodland is 8 m^2 ha^{-1} (Eamus et al., 2013).

134   The second eddy covariance site contains two species of trees: widely spaced and

135 tall *Corymbia opaca* trees above a matrix of hummock grass (Spinifex, *Triodia schinzii*)

136 and small patches of Mulga (*A. sericophylla*, *A. melleodora* and *A. aptaneura*) that contain

137 an understorey of herbs and tussock grasses (*Aristida* spp., *Eremophila latrobei* subsp.

138 *glabra*, *Eragrostis eriopoda* subsp. *red earth*, *Paraneurachne muelleri* and *Psydrax*

139 *latifolia*). Although the distribution of *T. schinzii* does not substantially overlap with

140 Mulga, *C. opaca* trees were present in both habitats. Representing only 0.4 % cover

141 (basal area of 0.21 m^2 ha^{-1}), *C. opaca* are found predominantly in the open savanna,

142 although they are found occasionally in the isolated small Mulga patch close to the EC

143 tower within in the *Corymbia* savanna. Soil texture is sandier in the *Corymbia* savanna

144 (loamy sand) than in the Mulga woodland (sandy loam). Soil organic matter is less than

145 1% at both sites. In the *Corymbia* savanna, the energy balance ratio $(H + LE) / (R_n - G)$

146   was 0.97 ± 0.005 (January 2013–July 2014), wherein H is sensible heat flux, LE is latent

147   heat flux, R_n is net radiation and G is ground heat flux. Over the same period in the Mulga

148   woodland, the energy balance ratio was 0.89 ± 0.005. The Bowen ratio (H/LE) was large

149   at both sites: 37.5 (range 0.78–408) in the Mulga woodland and 37.9 (0.23–511) in the

150   *Corymbia* savanna.

151   Long-term annual average precipitation (1987–2014) at the nearest meteorological

152   station (Territory Grape Farm, 18 km due south of the *Corymbia* savanna site) is 320.7

153   mm (http://www.bom.gov.au). The monsoon tropics of Australia are defined by the

154   receipt of 85% of annual precipitation during the November–April monsoon season

155   (Bowman et al., 2010), which places these sites within the monsoon zone on average

156   (Cleverly et al., 2013a). However, during the first 16 months of this study (August 2012–

157   November 2013), very little rain was received and there was consequently negligible

158   grassy understorey, in contrast to the extensive understorey that was present during the

159   land sink anomaly of 2011 (Eamus et al., 2013).

160

161   **2.2. Eddy covariance data**

162   Eddy covariance analyses of net ecosystem photosynthesis (NEP) and

163   evapotranspiration (ET) were used as measures of net C uptake and ecosystem water use.

164   In the eddy covariance method, ET is determined from the covariance between vertical

165   wind speed (w) and specific humidity (q): $ET = <w'q'>/\rho_w$, where $<>$ represents an

166   average in time and the prime operator represents the deviation from a mean: $q' = <q> -$

167   q_i. Similarly, NEP was taken to be the negative covariance between w and [CO_2] (c):

168    $NEP = -<w'c'>$. By this definition, NEP is positive during C uptake (i.e., photosynthesis,

169   C sink) and negative for net C emissions (C source). The trade-off between C uptake and

170   ET was represented by eWUE, which was calculated as the ratio of NEP and ET. Because

171   of non-linearity at very small values of ET, eWUE was determined only when ET was

172   larger than 0.2 mm d^{-1}.

173   Both tower sites are part of the OzFlux Network (Cleverly, 2011; Cleverly, 2013).

174   The 90% flux footprint (Kljun et al., 2004) under turbulent conditions extended 200–300

175   m to the southeast of either tower, although variability in roughness length across the

176   *Corymbia* savanna interferes with the reliability of footprint estimates at that site. In the

177   *Corymbia* savanna, approximately 25% of the flux footprint covered the *Corymbia*

178   savanna, while the remaining 75% of the footprint was located over the small Mulga patch

179   that included *Acacia*, *Corymbia* and tussock grasses. The trees nearest the tower in the

180   open *Corymbia* savanna are *Acacia* with a canopy height of 4.85 m, in contrast to the 6.5

181   m tall *Acacia* in the Mulga woodland. Thus, measurements were made over the *Corymbia*

182   savanna at a slightly lower height (9.85 m) than above the Mulga woodland (11.6 m,

183   Cleverly et al., 2013a). Where possible, the instruments on each tower were the same

184   (e.g., Campbell Scientific CSAT3) or only different in the model of sensor (e.g., Kipp &

185   Zonen CNR1 *v*. CNR4, Li-Cor 7500 *v*. 7500A), in which the newer models were used in

186   the *Corymbia* savanna.

187   All estimates of error were determined as the standard error (s.e. $= \sigma / n^{0.5}$, where σ

188   is the standard deviation and n is sample size).

189

190   **2.2.1. Quality control, corrections and gap-filling**

191   Quality control of meteorological and flux measurements (QA/QC) was performed

192   on both towers as described in Eamus et al. (2013). Briefly, QA/QC procedures included

193   spike detection and removal, range checks that include rejection of measurements when

194   the wind was from a 90° arc behind the sonic anemometer (CSAT3) and tower (10% of

195   observations, only during the passage of frontal systems that generate advection and

196   negative fluxes of LE; Beringer and Tapper, 2000), and filtering for bad measurements of

197   humidity from the IRGA in comparison to a slow-response sensor. Corrections included

198   2-dimensional coordinate rotation (Wesely, 1970), frequency attenuation correction for

199   time averaging and sensor displacement (Massman and Clement, 2004), conversion of

200   virtual to actual sensible heat flux (Campbell Scientific Inc., 2004; Schotanus et al., 1983),

201   correction for flux-density effects (WPL; Webb et al., 1980) and storage of heat in the soil

202   above the ground heat flux plates. Corrections and QA/QC steps were performed using

203   OzFluxQC and the OzFluxQC Simulator, both in version 2.8.5 and available online (e.g.,

204   Cleverly and Isaac, 2015). Gaps in fluxes were filled using a self-organising linear output

205   (SOLO) that was trained on a self-organising feature map (SOFM) of meteorological (net

206   radiation, air temperature, vapour pressure deficit, specific humidity) and soil

207   measurements (G, soil temperature, soil moisture content at the surface) (Eamus et al.,

208   2013). SOLO is a statistical artificial neural network (ANN) and was chosen for its

209   resistance to overtraining (Hsu et al., 2002), ability to simulate fluxes (Abramowitz et al.,

210   2006), and small RMSE relative to feed forward ANNs (Eamus et al., 2013).

211   In contrast to gaps in the flux measurements, two types of gaps were identified in

212   the meteorological data: those that were due to measurement over-ranging on the

213   datalogger and those that occurred during system maintenance. Over-ranging was

214   identified in the measurement of solar radiation during periods when reflection from a

215   cloud face generated large (> 1200 W m^{-2}) radiant fluxes. To avoid underestimation bias

216   in these cases, gaps in 30-minute solar (R_s) and net (R_n) radiation were filled from the

217   measured value in each minute that did not report an over-ranging error (26–29 one-

218   minute values). These gaps first occurred during the summer 2012–2013 at the *Corymbia*

219   savanna site, after which modifications to the datalogger prevented re-occurrence of solar

220   spike gaps.

221   System maintenance gaps were typically 30–300 minutes and did not coincide

222   among sites. Filling of gaps in the meteorological variables that were used as predictors

223   for gap filling of fluxes was performed using several methods: 1) linear interpolation, 2)

224   replacement of measurements from the companion tower, and 3) SOLO-SOFM trained on

225   measurements from the paired tower. Gaps in meteorological measurements were filled

226   using the method that produced the smallest disjunction at gap boundaries.

227

228   2.3. Trends in satellite derived enhanced vegetation index (EVI) for the two sites

229   The moderate resolution imaging spectroradiometer (MODIS) enhanced vegetation

230   index (EVI) is sensitive to vegetation "greenness" (i.e., chlorophyll content) and structural

231   properties (e.g., LAI, canopy type, plant physiognomy, canopy architecture) (Huete et al.,

232   2002). Thus, the satellite product MODIS EVI was used in this study to assess structural

233   and functional responses of the vegetation. The MOD13Q1 product was retrieved from

234   the satellite at a temporal resolution of 16 days and a spatial resolution of 250 m, and then

235   the values were composited into a single 9×9 pixel centred on each tower (2.25 km

236   resolution, only pixels that passed QA at 100% were used). The MODIS satellite was

237   launched in 2000, and we present the entire record to provide context for the ecosystem

238   dynamics observed over this two-year study.

239

240   2.4. ^{13}C foliar stable isotopes

241   To compare leaf-scale intrinsic WUE (WUE$_i$) at small spatial scales within the

242   *Corymbia* savanna, leaf samples were collected in September 2013 for analysis of the

243   stable isotope ratio of C ($\delta^{13}C$). Mature leaves of *Corymbia opaca* and *Acacia* trees were

244   collected from three habitats within the *Corymbia* savanna. The first habitat was from the

245   *Corymbia* savanna *per se*; the second habitat was the small Mulga patch close to the EC

246 tower within the *Corymbia* savanna; the third habitat was the transition between the small

247 Mulga patch and the *Corymbia* savanna. For comparison with *Acacia* sampled within the

248 *Corymbia* savanna, $\delta^{13}C$ of bulk leaf tissue was also measured in the Mulga woodland

249 from two replicate branches of three replicate trees of *Acacia*.

250 In *Corymbia*, three leaves from different branches were collected. Each leaf was

251 ground and subsampled to obtain three representative independent values per tree.

252 Likewise, *Acacia* phyllodes were sampled from three different branches, although several

253 phyllodes were combined from each branch due to their small size. The C isotopic

254 composition was measured using a Picarro G2121-i Analyser for Isotopic CO_2 (Picarro

255 Inc., Santa Clara CA USA). Atropine and acetanilide were used as internal reference

256 standards and calibrated against international measurement standards sucrose (IAEA-CH-

257 6, $\delta^{13}C_{VPDB} = -10.45$ ‰), cellulose (IAEA-CH-3, $\delta^{13}C_{VPDB} = -24.72$ ‰) and graphite

258 (USGS24, $\delta^{13}C_{VPDB} = -16.05$ ‰). Values of $\delta^{13}C$ in bulk leaf samples represent an

259 integrated value of C_i/C_a (i.e., the ratio of internal leaf and atmospheric CO_2 density)

260 during the entire age of the leaf.

261

262 **3. Results**

263 **3.1. Water fluxes: daily, seasonal and annual precipitation**

264 Daily rainfall across the two-year period showed minimal differences between the

265 Mulga woodland and *Corymbia* savanna sites (Fig. 1a, b). Rainfall in both years was

266 concentrated between November and early May, although both sites received about 12

267 mm of rain in July 2014. During the first year of this study (2013–2014), rainfall during

268 the monsoon season (November–April) was 71 and 74% of total annual rainfall for that

269 year in the Mulga woodland and *Corymbia* savanna, respectively. In the following year,

270 rainfall during the monsoon season was 92% of total annual rainfall at both sites.
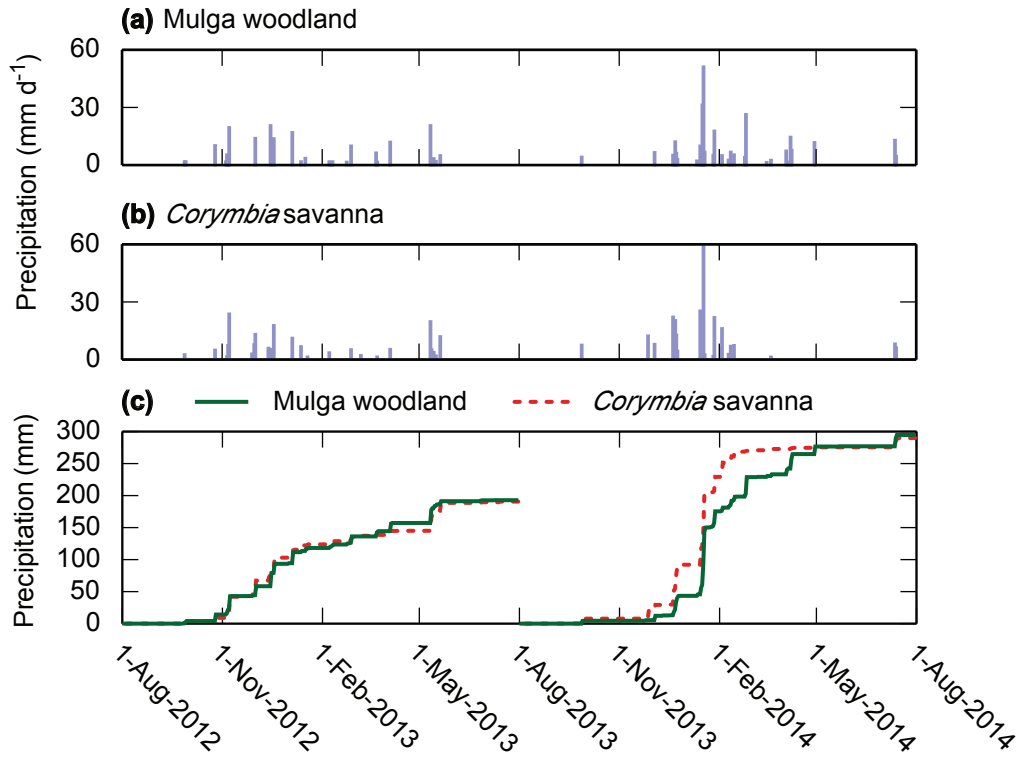
Figure 1. Daily (a, b) and cumulative (c) precipitation in the Mulga woodland (a, solid line c) and the *Corymbia* savanna (b, broken line c).

271 Although these sites are within the monsoon zone on average (Cleverly et al., 2013a), the

272 monsoon did not penetrate inland to the location of these sites in the first year of the

273 present study (August 2012–July 2013). Due to the proximity between sites, annual

274 rainfall did not differ in either of the two years of the present study. Likewise, due to

275 cross-correlation between precipitation

276 *versus* temperature (maximum, mean,

277 minimum), solar radiation and vapour

278 pressure deficit (Cleverly et al., 2013a),

279 meteorological conditions were equivalent

280 across sites (data not shown).

281   In the 2010–2011 hydrological year

Table 1. Summary of rainfall and net ecosystem productivity (NEP) for four years of study at the Mulga woodland. Data for 2010–2012 from Eamus *et al*. (2013) and Cleverly *et al*. (2013a). Data for 2012–2013 from this study.

Year	Rainfall (mm y^{-1})	NEP (g C m^{-2} y^{-1})
2010–2011	565	259
2011–2012	184	−4
2012–2013	193	−25
2013–2014	295	12

282 (August–July), annual rainfall (565 mm) was significantly larger than the long-term

283 average of 320.7 mm (Table 1). In contrast, annual rainfall was smaller than average in

284 hydrological years 2011–2013 (Table 1). During the first year of this study (August

12

285   2012–July 2013), annual rainfall was approximately 40% less than the long-term average

286   (192.8 and 190.6 mm in the Mulga woodland and *Corymbia* savanna, respectively). In the

287   second year of this study (2013–2014), rainfall was 294.6 and 289.8 mm in the Mulga

288   woodland and *Corymbia* savanna, respectively (approximately 8% below the long-term

289   average). Monthly patterns and cumulative annual (August–July) rainfall in the first year

290   of study were almost identical at the two sites (Fig. 1c). In contrast there was more rain

291   earlier in the second hydrologic year (November 2013–February 2014) at the *Corymbia*

292   savanna than the Mulga woodland, although annual totals for the two sites did not differ.

293

294   **3.2. Water fluxes: evapotranspiration**

295   Patterns in daily ET were similar across the two-year study at both sites (Fig. 2a)

296   and closely followed those observed for rainfall. Daily ET at both sites was negligible

297   during those periods when daily rainfall was zero for more than two weeks (e.g., August
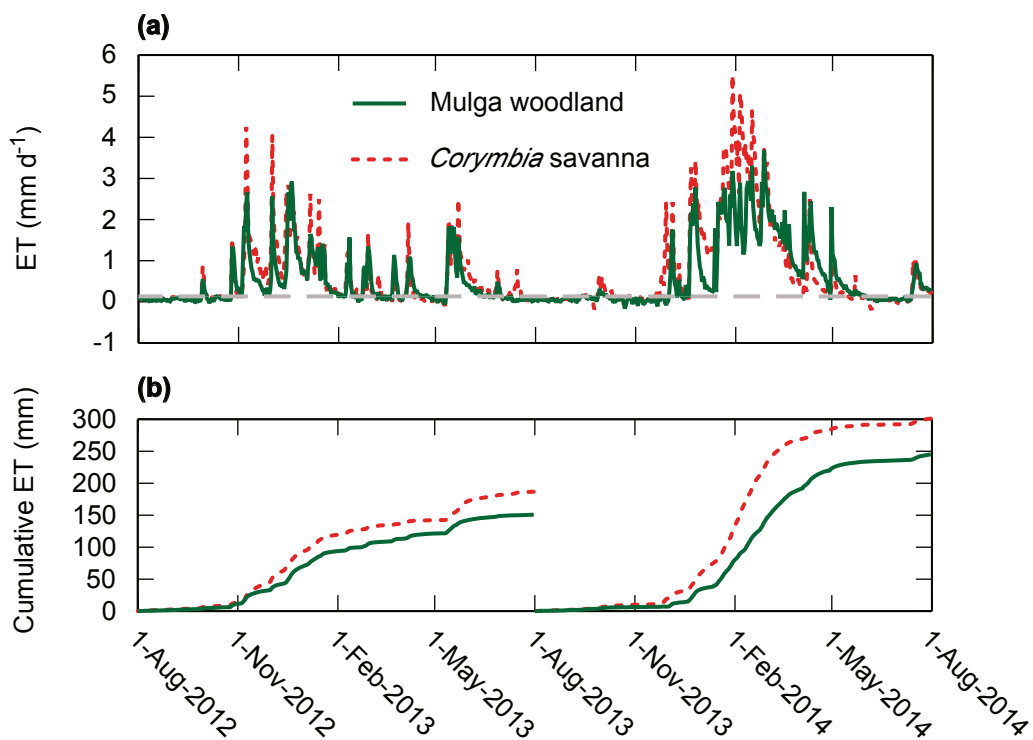
Figure 2. Daily (a) and cumulative (b) evapotranspiration (ET) in the Mulga woodland (solid
line) and the *Corymbia* savanna (broken line).

298   2012 and 2013, June 2014). Maximum rates of daily ET from the *Corymbia* savanna were

299   either equal to or frequently larger (by up to approximately 80%) than those from the

300   Mulga woodland (Fig. 2a). Summer total and maximum daily rates of ET were larger in

301   the second summer than the first at both sites. As with rainfall, 73 and 88% of ET was

302   lost from the Mulga woodland during the first and second monsoon seasons, respectively.

303   Likewise in the *Corymbia* savanna, 71 and 91% of ET was lost during the respective

304   monsoon seasons.

305   In both hydrologic years (August 2012–July 2014), patterns of cumulative ET

306   were broadly similar at the two sites, but with a consistent difference in the total amount

307   of ET (Fig. 2b). Moreover, the annual sum of ET was smaller for the Mulga woodland

308   than the *Corymbia* savanna in both years. The annual total ET for the *Corymbia* savanna

309   was 96 and 110% of annual rainfall in each year (2012–2013 and 2013–2014,

310   respectively), but in the Mulga woodland the annual sum of ET was approximately 80%

311   of total rainfall in both years (cf. Figs. 1c and 2b). Immediately following precipitation,

312   there were larger pulses of ET from the *Corymbia* savanna than from the Mulga woodland

313   (cf. Figs. 1c and 2a). These short imbalances were more prominent in the second year,

314   when ET was 110% of precipitation in the *Corymbia* savanna.

315

316   **3.3. Carbon fluxes: net productivity and water-use efficiency**

317   In contrast to the very similar patterns in daily ET at both sites, patterns in daily

318   NEP differed substantially between the two sites (Fig. 3a). During the winter and early

319   spring (August–October) of 2012, the Mulga woodland was a small sink (NEP = 0.1 to 0.3

320   g C m^{-2} d^{-1}), but the *Corymbia* savanna was a moderate source for C (NEP = −0.6 to −0.3

321   g C m^{-2} d^{-1}). This pattern was repeated in the second winter/early spring (June–August

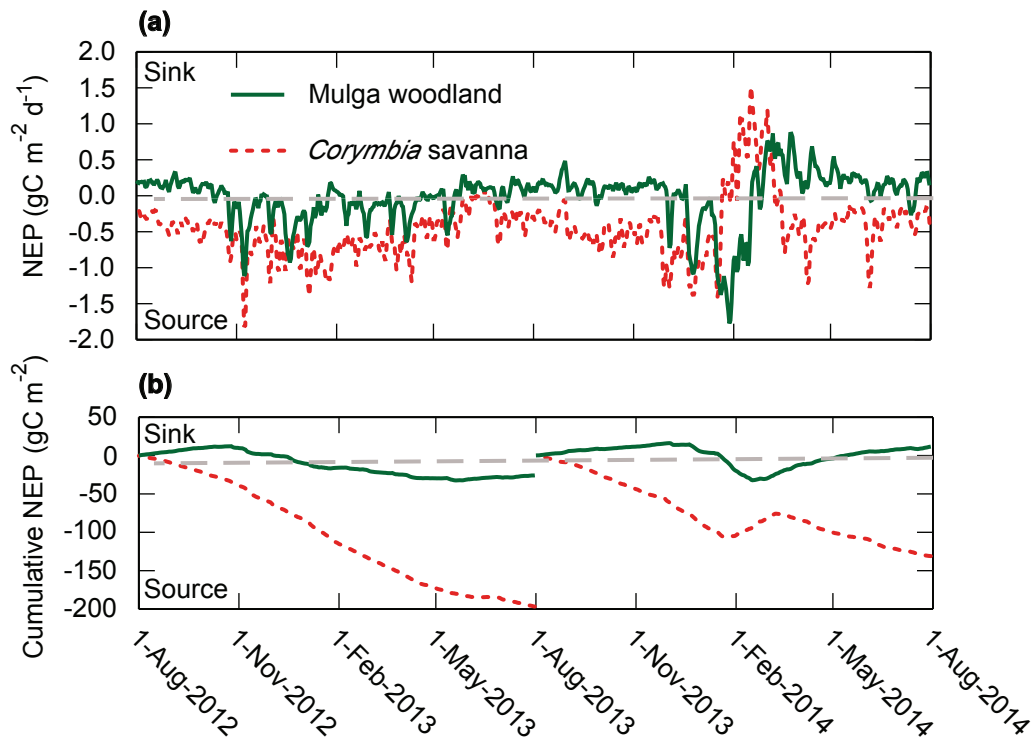322   2013). The *Corymbia* savanna remained a moderate-to-strong source (NEP = −1.75 to

Figure 3. Daily (a) and cumulative annual (b) net ecosystem productivity (NEP) in the Mulga woodland (solid line) and the *Corymbia* savanna (broken line). Daily values are shown as the 3-day running average. Values of NEP that are larger than zero (dashed line) represent carbon uptake.

323   -0.5 g C m^{-2} d^{-1}) between November 2012 and January 2014, with the exception of a

324   short period during June 2013 when the *Corymbia* savanna became C neutral (uptake

325   equalled release) (Fig. 3a). The *Corymbia* savanna was a sink for C (maximum daily NEP

326    $= 1.5$ g C m^{-2} d^{-1}) for approximately 6 weeks in the summer of 2014 (late January to early

327   March). The Mulga was a moderate-to-large C source for the spring and early summer of

328   2014 and became a moderate sink (maximum NEP $= 0.75$ g C m^{-2} d^{-1}) in late summer and

329   autumn of 2014 (Fig. 3a).

330   During summer in the *Corymbia* savanna, the pulse of productivity was rapid and

331   large following the largest storm in the two years of study (> 100 mm in January 2014; cf.

332   Figs. 1 and 3a), and this was due to the dominant cover of C$_4$ grasses (90%). By contrast

333   in the Mulga woodland, productivity was limited during the summer, acting as a source

334   for several weeks until late summer and early autumn of 2014 (Fig. 3a). In contrast, both

335   sites were a C source in January 2013 (Fig. 3a). During this time, ecosystem respiration at

15

336 night was similarly small in the Mulga woodland and *Corymbia* savanna (Fig. 4).

337 However, during the sunlit hours, NEP

338 diverged between the two sites. Even

339 though the Mulga woodland was a net

340 C source, small rates of NEP were

341 observed in the morning before

342 declining well before sundown (Fig.

343 4). By contrast, NEP declined during

344 sunlit hours in the *Corymbia* savanna,

345 illustrating that C losses were

346 enhanced in the daytime (Fig. 4).

347   Cumulative annual NEP in

348 both hydrologic years showed the

Figure 4. Daily cycle of NEP. Values represent hourly average ± standard error (s.e.) during January 2013.

349 *Corymbia* savanna to be a strong source (cumulative NEP = −197 and −131 g C m^{-2} y^{-1}

350 for the first and second years, respectively; Fig. 3b). In contrast, the Mulga woodland was

351 a small source (−26 g C m^{-2} y^{-1}) in the first hydrologic year but a small sink (12 g C m^{-2}

352 y^{-1}) in the second year. It wasn't until the occurrence of a wet summer that the Mulga

353 woodland again became a moderate-to-strong sink (0.9 g C m^{-2} d^{-1}), although annual C

354 uptake was considerably less than that observed in the 2010–2011 anomaly (12 *versus* 259

355 g C m^{-2} y^{-1}), reflecting the non-linear response of NEP to total annual rainfall in this

356 system. The trend in cumulative NEP at the two sites diverged in early March 2014, with

357 the *Corymbia* savanna reverting to a source for the remaining five months of the study and

358 the Mulga continuing as a net sink (Fig. 3b).

359   In the *Corymbia* savanna, eWUE was negative (negative because respiratory loss

360 exceeded photosynthetic C gain) for most of the two years of study (Fig. 5) and was more
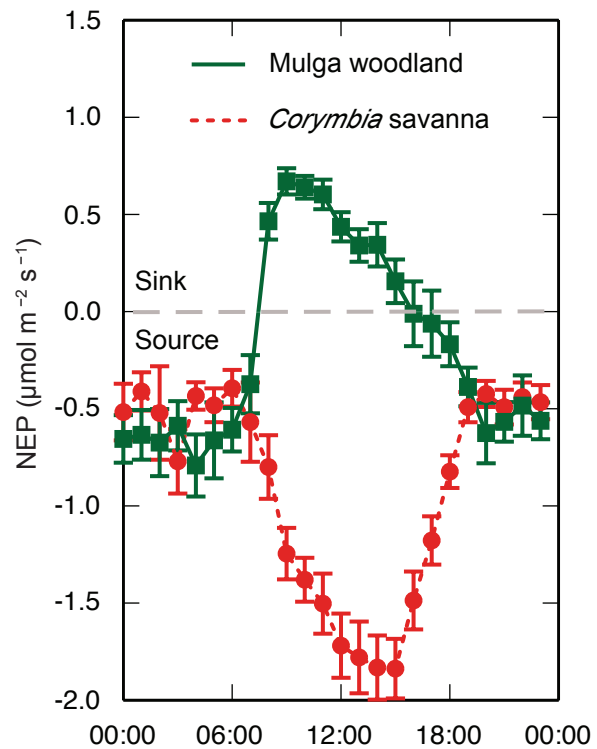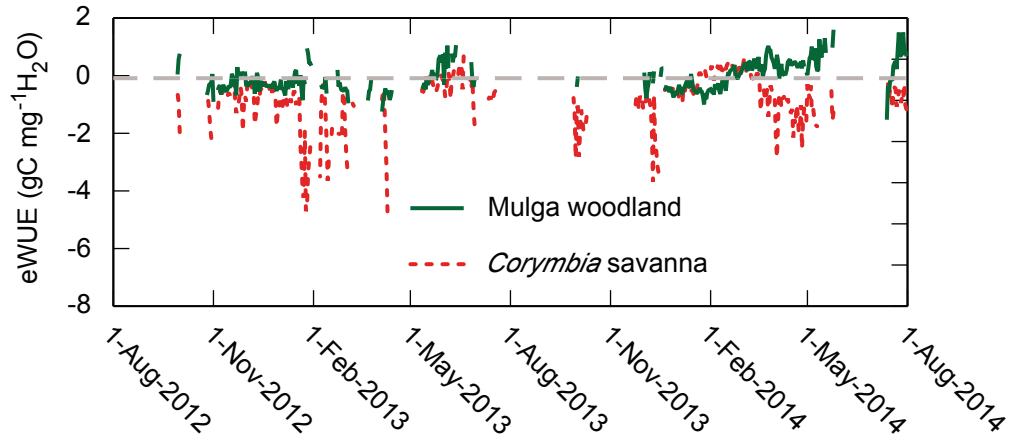
Figure 5. Daily ecosystem water use efficiency (eWUE). Values were determined as NEP∕ET and shown for days when ET > 0.2 mm d^{-1}. Values above zero (dashed line) represent photosynthetic eWUE, while increasingly negative values of eWUE represent increasing values of respiratory eWUE.

361 negative in the first hydrologic year than the second. Periods of very small positive or

362 slightly negative eWUE for the *Corymbia* coincided with the rainfall of November 2012–

363 February 2013, May 2013 and January–March 2014. In contrast, the Mulga woodland

364 maintained near-zero values of eWUE in both years. In the Mulga woodland, eWUE

365 increased with time since rainfall during each year's autumn (March–May, Fig. 5).

366

367 **3.4. Trends in enhanced vegetation index and foliar ^{13}C stable isotope contents**

368   MODIS EVI peaked at the study sites in five of 13 years since the launch of the

369 satellite: March 2000, April 2001, April 2007, March 2010 and March 2011 (Fig. 6). In a

370 given year, neither ecosystem

371 consistently responded to precipitation

372 with more production of green tissue

373 than the other (Fig. 6). While MODIS

374 EVI was generally larger in the Mulga

375 woodland than the *Corymbia* savanna,

376 two periods (2004 and 2010) when this

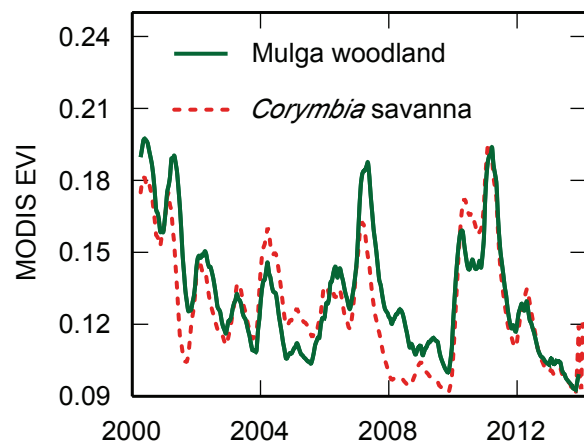377 pattern was reversed are apparent (Fig.

Figure 6. MODIS enhanced vegetation index (EVI) as a four-month running average.

378   6). Note that during the first year of this study (2012–2013), MODIS EVI values were the

379   smallest on record for the Mulga woodland and as small as previous minima in the

380   *Corymbia* savanna (2008, 2009).

381   In *Acacia* phyllodes, $\delta^{13}C$ values averaged −27.9‰ and did not differ substantially

382   across the two sites and in the three

383   habitats sampled within the *Corymbia*

384   savanna. By contrast, $\delta^{13}C$ in *Corymbia*

385   *opaca* leaves declined substantially

386   across habitats (Fig. 7). Leaf $\delta^{13}C$ of the

387   *Corymbia* trees declined in the sequence:

388   *Corymbia* trees in the Mulga patch

389   within the *Corymbia* savanna >

390   *Corymbia* trees in the transition between

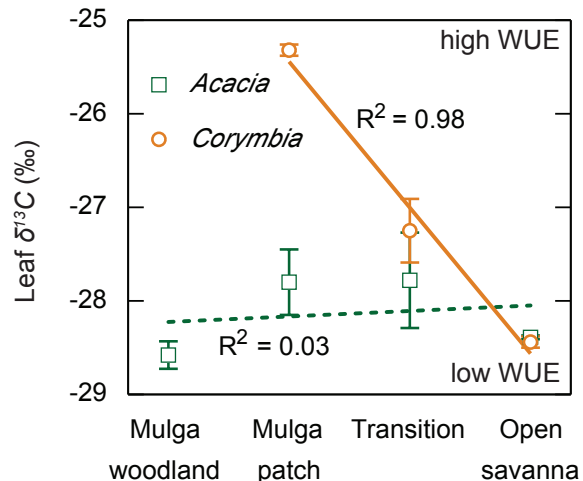391   the *Acacia* patch and open *Corymbia*

Figure 7. Carbon stable isotope ratio ($\delta^{13}C$) of *Acacia* (squares) and *C. opaca* (circles) leaves in the Mulga woodland and across three habitats (Mulga patch, open savanna, transition) within the *Corymbia* savanna. Symbols show mean ± s.e.

392   savanna > *Corymbia* trees in the extensive open savanna (Fig. 7). Leaf $\delta^{13}C$ in *Corymbia*

393   was less negative than in *Acacia* phyllode in the Mulga patch (Fig. 7).

394

395   **4. Discussion**

396   **4.1. The 2011 anomaly and beyond**

397   Although measurements were not initiated in the *Corymbia* savanna until after the

398   conclusion of the land sink anomaly, C fluxes in subsequent years can only be explained

399   within the context of the land sink anomaly. Several lines of field-based evidence support

400   the conclusion (Le Quéré et al., 2014; Poulter et al., 2014) that Australian semi-arid

401   vegetation had a major role in the large global land sink anomaly of 2011. First, our field-

402   based studies of CO_2 fluxes in central Australia (Table 1; Eamus et al., 2013)

18

403   demonstrated that the Mulga woodland was indeed a large sink for C (2.6 t C ha^{-1} y^{-1}, 259

404   g C m^{-2} y^{-1}, Table 1) during that year (September 2010–August 2011; Eamus et al., 2013).

405   This sink formed in response to a disproportionate increase in gross primary production

406   (GPP, 7.9 t C ha^{-1} y^{-1}, 793 g C m^{-2} y^{-1}) relative to the moderate increase in ecosystem

407   respiration (Cleverly et al., 2013a). Second, the largest value of EVI since 2000 was

408   observed in hydrologic year 2010–2011 (Ma et al., 2013), which suggests as large a C sink

409   in the *Corymbia* savanna as in the Mulga woodland due to the close correlation between

410   EVI and GPP across Australia (Donohue et al., 2014; Ma et al., 2013; Ma et al., 2014).

411   Third, 2010–2011 was identified as having the largest rates of ET in the Ti Tree basin

412   since 1981 (Chen et al., 2014). Finally, the Gravity Recovery and Climate Experiment

413   satellite data recorded significant increases in the amount of water stored across the

414   Australian landmass in 2011 (Boening et al., 2012), coincident with the extremely large

415   La Niña conditions that dominated weather across Australia in that year.

416   During the land sink anomaly of 2011, rainfall at our sites was almost double the

417   long-term average (565 mm *versus* 320.7 mm, 1987–2014), resulting in very large rates of

418   ecosystem productivity in the Mulga woodland (Eamus et al., 2013) and the *Corymbia*

419   savanna (Fig. 6). Across a range of biomes, different combinations of rainfall,

420   temperature, solar radiation and vapour pressure deficit are the principle determinants of

421   NEP and GPP (Baldocchi, 2008; Baldocchi and Ryu, 2011; Kanniah et al., 2010; van Dijk

422   et al., 2005; Zha et al., 2013). It is apparent that inter-annual differences in rainfall are the

423   principle causes of interannual differences in sink strength for the Mulga woodland (Table

424   1), in strong agreement with multiple other arid and semiarid biomes (Barron-Gafford et

425   al., 2012; Chen et al., 2014; Flanagan and Adkinson, 2011; Huxman et al., 2004; Ma et al.,

426   2012) but in marked contrast to boreal forests, tropical montane forests, temperate mesic

427   deciduous forests and tropical mesic savannas, where temperature, solar radiation and the

428 length of the growing season are the principal factors limiting NEP (Baldocchi, 2008;

429 Dunn et al., 2007; Keenan et al., 2014; Luyssaert et al., 2007; Ma et al., 2013; Whitley et

430 al., 2011; Zha et al., 2013). We now discuss the question: did this anomaly persist into

431 2012–2014 for our two study sites?

432 The productivity pulse of 2011 did not persist in either ecosystem following the

433 conclusion of the land sink anomaly. Productivity declined in the Mulga woodland by

434 July 2011, which was four months following the end of the summer rains (Cleverly et al.,

435 2013a; Eamus et al., 2013), and the Mulga woodland was effectively C neutral (i.e., near

436 zero within the limits of measurement uncertainty) in the three following years (2012–

437 2014). The ratio of GPP to ecosystem respiration fell between 2011 and 2012, reflecting a

438 two-fold decline in annual GPP (Cleverly et al., 2013a) and a four-fold decline in the

439 seasonal peak of daily GPP (Ma et al., 2013). Similarly, there was little evidence of

440 productivity in the *Corymbia* savanna during the first nine months of the current study

441 (August 2012–May 2013). In pyrophytic landscapes such as the *Corymbia* savanna, large

442 amounts of fuel can accumulate following very wet periods (King et al., 2013; Schlesinger

443 et al., 2013). However, large rates of C loss from this biome during subsequent dry years

444 imply a rapid loss of fuel load via photodegradation. Thus, *Corymbia* savannas that do

445 not burn in the first few years following very wet conditions are less likely to burn

446 thereafter.

447

448 **4.2. *Corymbia* savanna *versus* Mulga woodland**

449 In this section, we address the question: how do current behaviours of the Mulga

450 woodland (in terms of CO_2 and water fluxes) compare to those of an adjacent, floristically

451 different, *Corymbia* savanna?

452   Some of the ET excess in the *Corymbia* savanna in the second year of study (ET =

453   110% of precipitation) arose from precipitation that fell during the first year but

454   contributed to second-year ET, while the remainder may illustrate the opportunistic use of

455   groundwater by *Corymbia* trees in the open savanna during short periods of cloud cover,

456   cool temperatures, and low VPD that accompany rainfall. What was perhaps surprising

457   was the continued ET deficit in the Mulga woodland (about 80% of annual rainfall) in the

458   very wet (2011) year (Eamus et al., 2013) and the subsequent the dry years, with little

459   apparent use of water that was carried-over in soil storage. However, the abundant

460   sunshine and soil moisture availability during the summer of 2013–2014 may suggest that

461   ET was limited by stomatal responses to high temperature and large VPD (Cleverly et al.,

462   2013b) rather than energy or water availability. Thus, recharge and discharge of soil

463   moisture storage (and the ratio of ET to precipitation) vary on longer timescales than the

464   scope of our measurements, in contrast to the intra-annual carry-over of water from the

465   wet season into the cool season observed in North American drylands (Hastings et al.,

466   2005).

467   The interplay between drought tolerance and resilience resulted in a near-neutral

468   annual C balance in the Mulga woodland (Fig. 3 and Cleverly et al., 2013a), whereas the

469   C cycle in the *Corymbia* savanna was dominated by large C losses (Fig. 3). Two reasons

470   may be postulated to explain the difference in C balance of the two sites. First, *Acacia* has

471   a suite of traits that are indicative of a high degree of drought tolerance compared to

472   *Corymbia*: larger wood density, smaller specific leaf area (SLA, ratio of leaf area to leaf

473   dry mass) and larger Huber value (ratio of sapwood cross-sectional area to leaf area)

474   (O'Grady et al., 2009). Large wood densities are strongly correlated with enhanced

475   resistance to xylem embolism, reduced soil-to-leaf hydraulic conductance and small

476   transpiration rates (Wright et al., 2006; Zhang et al., 2009), while a small SLA correlates

477 with an ability to tolerate lower (more negative) canopy water potentials. As a result,

478 small rates of productivity in the Mulga woodland were sufficient for maintaining C

479 neutrality. Second, woody plants dominate the Mulga woodland, whereas the contribution

480 of *Acacia* and *Corymbia* to the cover, basal area and LAI of the *Corymbia* savanna is

481 small relative to the extensive C_4 grasses. We propose that the large amount of standing

482 dead biomass in the *Corymbia* savanna (accumulated during the 2011 anomaly) was

483 subject to physical fragmentation by photodegradation (i.e., in the presence of light, e.g.

484 Fig. 4, and absence of soil moisture; Rutledge et al., 2010; Vanderbilt et al., 2008).

485

486 **4.3. Ecosystem-scale water use efficiency (eWUE) and small-scale differences in**

487 **foliar WUE (WUE$_i$)**

488   By delaying production until the autumn of 2014, eWUE in the Mulga woodland

489 was larger than in the *Corymbia* savanna. In addition to the traits of drought tolerance,

490 which are correlated to large WUE, the large foliar N content of the nitrogen fixing *Acacia*

491 allows for significant resource substitution, whereby larger-than-expected rates of

492 photosynthesis can be sustained in arid environments through preferential allocations of

493 nitrogen to Rubisco (Taylor and Eamus, 2008). When stomatal conductance and

494 transpiration rates decline in response to large VPD, resource substitution results in large

495 eWUE. Further, spatial variability in soil properties (especially the distribution of the

496 hardpan) restricts soil moisture availability (Chen et al., 2014) and contributes to large

497 values of eWUE in the Mulga woodland.

498   It is important to note that the eWUE of the Mulga woodland consistently showed

499 that photosynthetic C uptake exceeded respiratory loss per unit ET during the early or late

500 summer and autumn of both years, as previously observed by Eamus et al. (2013). The

501 very low values of eWUE in the *Corymbia* savanna imply that C source strength was

502   maintained regardless of moisture status, thus eWUE became much more negative during

503   dry periods than eWUE in the Mulga woodland (Fig. 5). These predominantly large,

504   negative values of eWUE (respiration exceeds C gain per unit ET) in the *Corymbia*

505   savanna are further symptomatic of photodegradation. Despite the differences in eWUE

506   between ecosystems and the plants that co-exist in them, eWUE in the Mulga woodland

507   and the *Corymbia* savanna showed large fluctuations between wet and dry periods that

508   reflected differences in the moisture requirements of photosynthesis, autotrophic and

509   microbial respiration and photodegradation.

510   In leaves of *Corymbia* across all three habitats, declining leaf $\delta^{13}C$ represents

511   increased access to water and declining WUE_i (Leffler and Evans, 1999; Zolfaghar et al.,

512   2014) and has been previously used to infer access to groundwater (Zolfaghar et al.,

513   2014). We interpret this as reflecting an increasing rooting depth of *Corymbia* trees

514   within the *Corymbia* savanna when moving into the extensive open savanna from the

515   Mulga patch. The potential for groundwater access by deeply rooted *Corymbia* in the

516   extensive savanna, where groundwater depth is approximately 8 m, is presumably large

517   and may explain the lower WUE_i of *Corymbia*, while the presence of an inferred hardpan

518   within the Mulga patch prevents access to the water table and hence an increased WUE_i

519   for *Corymbia* within the Mulga patch. The absence of any significant change in phyllode

520   $\delta^{13}C$ for the *Acacia* at any of the three locations within the *Corymbia* savanna reflects the

521   shallow rooting habit of *Acacia* (Pressland, 1975). More importantly, there was no

522   difference in foliar ^{13}C content of *Acacia* sampled from the Mulga woodland where

523   groundwater depth is known to exceed 50 m, further supporting the conclusion that access

524   to groundwater by Mulga within the *Corymbia* savanna is not occurring. The low values

525   of $\delta^{13}C$ in *Acacia* phyllodes are consistent with their anisohydric stomatal responses to soil

23

526   drying; that is, their stomata remain open even at very low water potentials (O'Grady et

527   al., 2009; Winkworth, 1973).

528

529   **5. Conclusions**

530   We have demonstrated that the large 2011 anomaly in terrestrial C uptake was

531   short-lived in the arid zone of central Australia. In the Mulga woodland, storage of soil

532   moisture within the root zone contributed to C neutrality (i.e., C sources were equivalent

533   to sinks) in the subsequent drier-than-average years by facilitating the delayed response of

534   productivity to precipitation. We also demonstrated that productivity in the Mulga

535   woodland was larger than that of the *Corymbia* savanna in the drier-than-average years of

536   the study and attributed this to the multiple drought tolerant attributes and the larger

537   potential for resource substitution of *Acacia* compared to *Corymbia*. Drought tolerance in

538   the Mulga woodland further restricted ET to 80% of precipitation in each year since 2010,

539   indicating that variations in soil moisture storage occur over very long timescales. In

540   contrast, ET from the *Corymbia* savanna was larger than precipitation in the near-average

541   rainfall year, illustrating that groundwater use by *Corymbia* occurred opportunistically

542   during wet periods. However, the *Corymbia* savanna was a strong source of CO_2 in drier-

543   than-average and near-average years due to photodegradation of the extensive grassy

544   understorey. Finally, we demonstrated that ecosystem water-use efficiency was larger in

545   the Mulga woodland than in the *Corymbia* savanna, while differences in leaf/phyllode

546    $\delta^{13}C$ between *Acacia* and *Corymbia* reflected differential access to groundwater and the

547   different rooting characteristics of these two tree species.

548

549

6. Acknowledgements

7. References

Abramowitz, G., Gupta, H., Pitman, A., Wang, Y., Leuning, R., Cleugh, H. and Hsu, K.L., 2006. Neural Error Regression Diagnosis (NERD): A tool for model bias identification and prognostic data assimilation. J. Hydrometeor. 7: 160–177.

Baldocchi, D., 2008. Breathing of the terrestrial biosphere: lessons learned from a global network of carbon dioxide flux measurement systems. Aust. J. Bot. 56: 1–26, DOI: 10.1071/BT07151.

Baldocchi, D.D. and Ryu, Y., 2011. A synthesis of forest evaporation fluxes – from days to years – as measured with eddy covariance. In: D.F. Levia, D. Carlyle-Moses and T. Tanaka (Editors), Forest Hydrology and Biogeochemistry: Synthesis of Past Research and Future Directions. Ecological Studies. Springer, Dordrecht, Netherlands, pp. 101–116, DOI: 10.1007/978-94-007-1363-5_5.

Ballantyne, A.P., Alden, C.B., Miller, J.B., Tans, P.P. and White, J.W.C., 2012. Increase in observed net carbon dioxide uptake by land and oceans during the past 50 years. Nature. 488: 70–73, DOI: 10.1038/nature11299.

Barron-Gafford, G.A., Scott, R.L., Jenerette, G.D., Hamerlynck, E.P. and Huxman, T.E., 2012. Temperature and precipitation controls over leaf- and ecosystem-level CO_2 flux along a woody plant encroachment gradient. Glob. Change Biol. 18: 1389–1400, DOI: 10.1111/j.1365-2486.2011.02599.x.

Beringer, J. and Tapper, N.J., 2000. The influence of subtropical cold fronts on the surface energy balance of a semi-arid site. J. Arid. Environ. 44: 437-450.

Boening, C., Willis, J.K., Landerer, F.W., Nerem, R.S. and Fasullo, J., 2012. The 2011 La Niña: So strong, the oceans fell. Geophysical Research Letters. 39, DOI: L19602 10.1029/2012gl053055.

Bowman, D., Boggs, G.S. and Prior, L.D., 2008. Fire maintains an *Acacia aneura* shrubland—*Triodia* grassland mosaic in central Australia. J. Arid. Environ. 72: 34–47, DOI: 10.1016/j.jaridenv.2007.04.001.

Bowman, D., Boggs, G.S., Prior, L.D. and Krull, E.S., 2007. Dynamics of *Acacia aneura-Triodia* boundaries using carbon (^{14}C and δ^{13}C) and nitrogen (δ^{15}N) signatures in soil organic matter in central Australia. Holocene. 17: 311–318, DOI: 10.1177/0959683607076442.

Bowman, D., Brown, G.K., Braby, M.F., Brown, J.R., Cook, L.G., Crisp, M.D., Ford, F., Haberle, S., Hughes, J., Isagi, Y., Joseph, L., McBride, J., Nelson, G. and Ladiges, P.Y., 2010. Biogeography of the Australian monsoon tropics. J. Biogeogr. 37: 201–216, DOI: 10.1111/j.1365-2699.2009.02210.x.

Breshears, D.D., Myers, O.B. and Barnes, F.J., 2009. Horizontal heterogeneity in the frequency of plant-available water with woodland intercanopy-canopy vegetation patch type rivals that occuring vertically by soil depth. Ecohydrology. 2: 503–519.

596   Calf, G.E., McDonald, P.S. and Jacobson, G., 1991. Recharge mechanism and
597 groundwater age in the Ti-Tree basin, Northern Territory. Aust. J. Earth Sci. 38: 299–306,
598 DOI: 10.1080/08120099108727974.

599   Campbell Scientific Inc., 2004. Open path eddy covariance system operator's
600 manual, Logan, UT, USA, pp. 60.

601   Campos, G.E.P., Moran, M.S., Huete, A., Zhang, Y., Bresloff, C., Huxman, T.E.,
602 Eamus, D., Bosch, D.D., Buda, A.R., Gunter, S.A., Scalley, T.H., Kitchen, S.G.,
603 McClaran, M.P., McNab, W.H., Montoya, D.S., Morgan, J.A., Peters, D.P.C., Sadler, E.J.,
604 Seyfried, M.S. and Starks, P.J., 2013. Ecosystem resilience despite large–scale altered
605 hydroclimate conditions. Nature. 494: 349–352, DOI: 10.1038/nature11836.

606   Chen, C., Eamus, D., Cleverly, J., Boulain, N., Cook, P., Zhang, L., Cheng, L. and
607 Yu, Q., 2014. Modelling vegetation water-use and groundwater recharge as affected by
608 climate variability in an arid-zone *Acacia* savanna woodland. J. Hydrol. 519: 1084–1096,
609 DOI: 10.1016/j.jhydrol.2014.08.032.

610   Cleverly, J., 2011. Alice Springs Mulga OzFlux site. OzFlux: Australian and New
611 Zealand Flux Research and Monitoring Network, hdl: 102.100.100/8697.

612   Cleverly, J., 2013. Ti Tree East OzFlux Site. OzFlux: Australian and New Zealand
613 Flux Research and Monitoring Network, hdl: 102.100.100/11135.

614   Cleverly, J., Boulain, N., Villalobos-Vega, R., Grant, N., Faux, R., Wood, C.,
615 Cook, P.G., Yu, Q., Leigh, A. and Eamus, D., 2013a. Dynamics of component carbon
616 fluxes in a semi-arid *Acacia* woodland, central Australia. J. Geophys. Res. Biogeosci. 118:
617 1168–1185, DOI: 10.1002/jgrg.20101.

618   Cleverly, J., Chen, C., Boulain, N., Villalobos-Vega, R., Faux, R., Grant, N., Yu,
619 Q. and Eamus, D., 2013b. Aerodynamic resistance and Penman-Monteith
620 evapotranspiration over a seasonally two-layered canopy in semiarid central Australia. J.
621 Hydrometeor. 14: 1562–1570, DOI: 10.1175/jhm-d-13-080.1.

622   Cleverly, J. and Isaac, P., 2015. OzFluxQC Simulator version 2.8.6. GitHub
623 respository, https://github.com/james-cleverly/OzFluxQC_Simulator, DOI:
624 10.5281/zenodo.13730.

625   Cook, P.G. and O'Grady, A.P., 2006. Determining soil and ground water use of
626 vegetation from heat pulse, water potential and stable isotope data. Oecologia. 148: 97–
627 107, DOI: 10.1007/s00442-005-0353-4.

628   Cox, P.M., Pearson, D., Booth, B.B., Friedlingstein, P., Huntingford, C., Jones,
629 C.D. and Luke, C.M., 2013. Sensitivity of tropical carbon to climate change constrained
630 by carbon dioxide variability. Nature. 494: 341–344, DOI: 10.1038/nature11882.

631   Donohue, R.J., Hume, I.H., Roderick, M.L., McVicar, T.R., Beringer, J., Hutley,
632 L.B., Gallant, J.C., Austin, J.M., van Gorsel, E., Cleverly, J.R., Meyer, W.S. and Arndt,
633 S.K., 2014. Evaluation of the remote-sensing-based DIFFUSE model for estimating
634 photosynthesis of vegetation. Remote Sens. Environ. 155: 349–365, DOI:
635 10.1016/j.rse.2014.09.007.

636   Dunn, A.L., Barford, C.C., Wofsy, S.C., Goulden, M.L. and Daube, B.C., 2007. A
637   long-term record of carbon exchange in a boreal black spruce forest: means, responses to
638   interannual variability, and decadal trends. Glob. Change Biol. 13: 577–590, DOI:
639   10.1111/j.1365-2486.2006.01221.x.

640   Eamus, D., Cleverly, J., Boulain, N., Grant, N., Faux, R. and Villalobos-Vega, R.,
641   2013. Carbon and water fluxes in an arid-zone *Acacia* savanna woodland: An analyses of
642   seasonal patterns and responses to rainfall events. Agric. For. Meteor. 182–183: 225–238,
643   DOI: 10.1016/j.agrformet.2013.04.020.

644   Flanagan, L.B. and Adkinson, A.C., 2011. Interacting controls on productivity in a
645   northern Great Plains grassland and implications for response to ENSO events. Glob.
646   Change Biol. 17: 3293–3311, DOI: 10.1111/j.1365-2486.2011.02461.x.

647   Harrington, G.A., Cook, P.G. and Herczeg, A.L., 2002. Spatial and temporal
648   variability of ground water recharge in central Australia: A tracer approach. Ground
649   Water. 40: 518–527, DOI: 10.1111/j.1745-6584.2002.tb02536.x.

650   Hastings, S.J., Oechel, W.C. and Muhlia-Melo, A., 2005. Diurnal, seasonal and
651   annual variation in the net ecosystem CO_2 exchange of a desert shrub community
652   (Sarcocaulescent) in Baja California, Mexico. Glob. Change Biol. 11: 927–939, DOI:
653   10.1111/j.1365-2486.2005.00951.x.

654   Hsu, K.-l., Gupta, H.V., Gao, X., Sorooshian, S. and Imam, B., 2002. Self-
655   organizing linear output map (SOLO): An artificial neural network suitable for hydrologic
656   modeling and analysis. Water Resour. Res. 38: 1302, DOI: 10.1029/2001wr000795.

657   Huete, A., Didan, K., Miura, T., Rodriguez, E.P., Gao, X. and Ferreira, L.G., 2002.
658   Overview of the radiometric and biophysical performance of the MODIS vegetation
659   indices. Remote Sens. Environ. 83: 195–213, DOI: 10.1016/s0034-4257(02)00096-2.

660   Huxman, T.E., Snyder, K.A., Tissue, D., Leffler, A.J., Ogle, K., Pockman, W.T.,
661   Sandquist, D.R., Potts, D.L. and Schwinning, S., 2004. Precipitation pulses and carbon
662   fluxes in semiarid and arid ecosystems. Oecologia. 141: 254–268, DOI: 10.1007/s00442-
663   004-1682-4.

664   Kanniah, K.D., Beringer, J. and Hutley, L.B., 2010. The comparative role of key
665   environmental factors in determining savanna productivity and carbon fluxes: A review,
666   with special reference to Northern Australia. Progress in Physical Geography. 34: 459–
667   490.

668   Keenan, T.F., Gray, J., Friedl, M.A., Toomey, M., Bohrer, G., Hollinger, D.Y.,
669   Munger, J.W., O/'Keefe, J., Schmid, H.P., Wing, I.S., Yang, B. and Richardson, A.D.,
670   2014. Net carbon uptake has increased through warming-induced changes in temperate
671   forest phenology. Nature Clim. Change. 4: 598–604, DOI: 10.1038/nclimate2253.

672   King, K.J., Cary, G.J., Bradstock, R.A. and Marsden-Smedley, J.B., 2013.
673   Contrasting fire responses to climate and management: insights from two Australian
674   ecosystems. Glob. Change Biol. 19: 1223–1235, DOI: 10.1111/gcb.12115.

675   Kljun, N., Calanca, P., Rotach, M.W. and Schmid, H.P., 2004. A simple
676 parameterisation for flux footprint predictions. Bound.-Lay. Meteor. 112: 503-523, DOI:
677 10.1023/b:boun.0000030653.71031.96.

678   Le Quéré, C., Peters, G.P., Andres, R.J., Andrew, R.M., Boden, T.A., Ciais, P.,
679 Friedlingstein, P., Houghton, R.A., Marland, G., Moriarty, R., Sitch, S., Tans, P., Arneth,
680 A., Arvanitis, A., Bakker, D.C.E., Bopp, L., Canadell, J.G., Chini, L.P., Doney, S.C.,
681 Harper, A., Harris, I., House, J.I., Jain, A.K., Jones, S.D., Kato, E., Keeling, R.F., Klein
682 Goldewijk, K., Körtzinger, A., Koven, C., Lefèvre, N., Maignan, F., Omar, A., Ono, T.,
683 Park, G.H., Pfeil, B., Poulter, B., Raupach, M.R., Regnier, P., Rödenbeck, C., Saito, S.,
684 Schwinger, J., Segschneider, J., Stocker, B.D., Takahashi, T., Tilbrook, B., van Heuven,
685 S., Viovy, N., Wanninkhof, R., Wiltshire, A. and Zaehle, S., 2014. Global carbon budget
686 2013. Earth Syst. Sci. Data. 6: 235–263, DOI: 10.5194/essd-6-235-2014.

687   Leffler, A.J. and Evans, A.S., 1999. Variation in carbon isotope composition
688 among years in the riparian tree *Populus fremontii*. Oecologia. 119: 311–319.

689   Loik, M.E., Breshears, D.D., Lauenroth, W.K. and Belnap, J., 2004. A multi-scale
690 perspective of water pulses in dryland ecosystems: climatology and ecohydrology of the
691 western USA. Oecologia. 141: 269–281.

692   Ludwig, J.A., Wilcox, B.P., Breshears, D.D., Tongway, D.J. and Imeson, A.C.,
693 2005. Vegetation patches and runoff-erosion as interacting ecohydrological processes in
694 semiarid landscapes. Ecology. 86: 288–297.

695   Luyssaert, S., Inglima, I., Jung, M., Richardson, A.D., Reichstein, M., Papale, D.,
696 Piao, S.L., Schulzes, E.D., Wingate, L., Matteucci, G., Aragao, L., Aubinet, M., Beers, C.,
697 Bernhofer, C., Black, K.G., Bonal, D., Bonnefond, J.M., Chambers, J., Ciais, P., Cook, B.,
698 Davis, K.J., Dolman, A.J., Gielen, B., Goulden, M., Grace, J., Granier, A., Grelle, A.,
699 Griffis, T., Grunwald, T., Guidolotti, G., Hanson, P.J., Harding, R., Hollinger, D.Y.,
700 Hutyra, L.R., Kolar, P., Kruijt, B., Kutsch, W., Lagergren, F., Laurila, T., Law, B.E., Le
701 Maire, G., Lindroth, A., Loustau, D., Malhi, Y., Mateus, J., Migliavacca, M., Misson, L.,
702 Montagnani, L., Moncrieff, J., Moors, E., Munger, J.W., Nikinmaa, E., Ollinger, S.V.,
703 Pita, G., Rebmann, C., Roupsard, O., Saigusa, N., Sanz, M.J., Seufert, G., Sierra, C.,
704 Smith, M.L., Tang, J., Valentini, R., Vesala, T. and Janssens, I.A., 2007. CO_2 balance of
705 boreal, temperate, and tropical forests derived from a global database. Glob. Change Biol.
706 13: 2509–2537, DOI: 10.1111/j.1365-2486.2007.01439.x.

707   Ma, J., Zheng, X.J. and Li, Y., 2012. The response of CO_2 flux to rain pulses at a
708 saline desert. Hydrol. Process. 26: 4029–4037, DOI: 10.1002/hyp.9204.

709   Ma, X., Huete, A., Yu, Q., Coupe, N.R., Davies, K., Broich, M., Ratana, P.,
710 Beringer, J., Hutley, L.B., Cleverly, J., Boulain, N. and Eamus, D., 2013. Spatial patterns
711 and temporal dynamics in savanna vegetation phenology across the North Australian
712 Tropical Transect. Remote Sens. Environ. 139: 97–115, DOI: 10.1016/j.rse.2013.07.030.

713   Ma, X., Huete, A., Yu, Q., Restrepo-Coupe, N., Beringer, J., Hutley, L.B.,
714 Kanniah, K.D., Cleverly, J. and Eamus, D., 2014. Parameterization of an ecosystem light-
715 use-efficiency model for predicting savanna GPP using MODIS EVI. Remote Sens.
716 Environ. 154: 253–271, DOI: 10.1016/j.rse.2014.08.025.

717   Martinez-Meza, E. and Whitford, W.G., 1996. Stemflow, throughfall and
718   channelization of stemflow by roots in three Chihuahuan desert shrubs. J. Arid. Environ.
719   32: 271–287.

720   Maslin, B.R. and Reid, J.E., 2012. A taxonomic revision of Mulga (*Acacia aneura*
721   and its close relatives: Fabaceae) in Western Australia. Nuytsia. 22: 129–167.

722   Massman, W. and Clement, R., 2004. Uncertainty in eddy covariance flux
723   estimates resulting from spectral attenuation. In: X. Lee, W. Massman and B. Law
724   (Editors), Handbook of Micrometeorology: A guide for Surface Flux Measurement and
725   Analysis. Atmospheres and Oceanographic Sciences Library. Kluwer Academic
726   Publishers, Dordrecht/Boston/London, pp. 67–100.

727   Nano, C.E.M. and Clarke, P.J., 2010. Woody-grass ratios in a grassy arid system
728   are limited by multi-causal interactions of abiotic constraint, competition and fire.
729   Oecologia. 162: 719–732, DOI: 10.1007/s00442-009-1477-8.

730   Nemani, R.R., Keeling, C.D., Hashimoto, H., Jolly, W.M., Piper, S.C., Tucker,
731   C.J., Myneni, R.B. and Running, S.W., 2003. Climate-driven increases in global terrestrial
732   net primary production from 1982 to 1999. Science. 300: 1560–1563, DOI:
733   10.1126/science.1082750.

734   Nix, H.A. and Austin, M.P., 1973. Mulga: a bioclimatic analysis. Tropical
735   Grasslands. 7: 9–20.

736   O'Grady, A.P., Cook, P.G., Eamus, D., Duguid, A., Wischusen, J.D.H., Fass, T.
737   and Worldege, D., 2009. Convergence of tree water use within an arid-zone woodland.
738   Oecologia. 160: 643–655, DOI: 10.1007/s00442-009-1332-y.

739   O'Grady, A.P., Cook, P.G., Howe, P. and Werren, G., 2006a. Groundwater use by
740   dominant tree species in tropical remnant vegetation communities. Aust. J. Bot. 54: 155–
741   171, DOI: 10.1071/bt04179.

742   O'Grady, A.P., Eamus, D., Cook, P.G. and Lamontagne, S., 2006b. Comparative
743   water use by the riparian trees *Melaleuca argentea* and *Corymbia bella* in the wet-dry
744   tropics of northern Australia. Tree Physiol. 26: 219–228.

745   Ogle, K. and Reynolds, J.F., 2004. Plant responses to precipitation in desert
746   ecosystems: integrating functional types, pulses, thresholds, and delays. Oecologia. 141:
747   282–294, DOI: 10.1007/s00442-004-1507-5.

748   Poulter, B., Frank, D., Ciais, P., Myneni, R.B., Andela, N., Bi, J., Broquet, G.,
749   Canadell, J.G., Chevallier, F., Liu, Y.Y., Running, S.W., Sitch, S. and van der Werf, G.R.,
750   2014. Contribution of semi-arid ecosystems to interannual variability of the global carbon
751   cycle. Nature. 509: 600–603, DOI: 10.1038/nature13376.

752   Pressland, A.J., 1975. Productivity and management of Mulga in south-western
753   Queensland in relation to tree structure and density. Aust. J. Bot. 23: 965–976, DOI:
754   10.1071/bt9750965.

755   Reid, N., Hill, S.M. and Lewis, D.M., 2008. Spinifex biogeochemical expressions
756 of buried gold mineralisation: The great mineral exploration penetrator of transported
757 regolith. Appl. Geochem. 23: 76–84, DOI: 10.1016/j.apgeochem.2007.09.007.

758   Reynolds, J.F., Kemp, P.R., Ogle, K. and Fernandez, R.J., 2004. Modifying the
759 'pulse-reserve' paradigm for deserts of North America: precipitation pulses, soil water, and
760 plant responses. Oecologia. 141: 194–210.

761   Reynolds, J.F., Stafford Smith, D.M., Lambin, E.F., Turner, B.L., Mortimore, M.,
762 Batterbury, S.P.J., Downing, T.E., Dowlatabadi, H., Fernandez, R.J., Herrick, J.E., Huber-
763 Sannwald, E., Jiang, H., Leemans, R., Lynam, T., Maestre, F.T., Ayarza, M. and Walker,
764 B., 2007. Global desertification: Building a science for dryland development. Science.
765 316: 847–851, DOI: 10.1126/science.1131634.

766   Rutledge, S., Campbell, D.I., Baldocchi, D. and Schipper, L.A., 2010.
767 Photodegradation leads to increased carbon dioxide losses from terrestrial organic matter.
768 Glob. Change Biol. 16: 3065–3074, DOI: 10.1111/j.1365-2486.2009.02149.x.

769   Scanlon, B.R., Keese, K.E., Flint, A.L., Flint, L.E., Gaye, C.B., Edmunds, W.M.
770 and Simmers, I., 2006. Global synthesis of groundwater recharge in semiarid and arid
771 regions. Hydrol. Process. 20: 3335–3370, DOI: 10.1002/hyp.6335.

772   Schlesinger, C., White, S. and Muldoon, S., 2013. Spatial pattern and severity of
773 fire in areas with and without buffel grass (*Cenchrus ciliaris*) and effects on native
774 vegetation in central Australia. Austral Ecol. 38: 831–840, DOI: 10.1111/aec.12039.

775   Schotanus, P., Nieuwstadt, F.T.M. and Debruin, H.A.R., 1983. Temperature-
776 measurement with a sonic anemometer and its application to heat and moisture fluxes.
777 Bound.-Lay. Meteor. 26: 81–93.

778   Schwinning, S., Sala, O.E., Loik, M.E. and Ehleringer, J.R., 2004. Thresholds,
779 memory, and seasonality: understanding pulse dynamics in arid/semi-arid ecosystems.
780 Oecologia. 141: 191–193, DOI: 10.1007/s00442-004-1683-3.

781   Taylor, D. and Eamus, D., 2008. Coordinating leaf functional traits with branch
782 hydraulic conductivity: resource substitution and implications for carbon gain. Tree
783 Physiol. 28: 1169–1177.

784   Thiry, M., Milnes, A.R., Rayot, V. and Simon-Coincon, R., 2006. Interpretation of
785 palaeoweathering features and successive silicifications in the Tertiary regolith of inland
786 Australia. J. Geol. Soc. 163: 723–736, DOI: 10.1144/0014-764905-020.

787   Tongway, D.J. and Ludwig, J.A., 1990. Vegetation and soil patterning in semiarid
788 mulga lands of Eastern Australia. Aust. J. Ecol. 15: 23–34, DOI: 10.1111/j.1442-
789 9993.1990.tb01017.x.

790   van Dijk, A., Dolman, A.J. and Schulze, E.D., 2005. Radiation, temperature, and
791 leaf area explain ecosystem carbon fluxes in boreal and temperate European forests. Glob.
792 Biogeochem. Cycle. 19: GB2029, DOI: 10.1029/2004gb002417.

793   Vanderbilt, K.L., White, C.S., Hopkins, O. and Craig, J.A., 2008. Aboveground
794   decomposition in arid environments: Results of a long-term study in central New Mexico.
795   J. Arid. Environ. 72: 696–709.

796   Webb, E., Pearman, G. and Leuning, R., 1980. Correction of flux measurements
797   for density effects due to heat and water-vapor transfer. Q. J. Roy. Meteor. Soc. 106: 85–
798   100.

799   Wesely, M.L., 1970. Eddy correlation measurements in the atmospheric surface
800   layer over agricultural crops. Ph.D. Dissertation Thesis, University of Wisconsin,
801   Madison, 102 pp.

802   Whitley, R.J., Macinnis-Ng, C.M.O., Hutley, L.B., Beringer, J., Zeppel, M.,
803   Williams, M., Taylor, D. and Eamus, D., 2011. Is productivity of mesic savannas light
804   limited or water limited? Results of a simulation study. Glob. Change Biol. 17: 3130–
805   3149, DOI: 10.1111/j.1365-2486.2011.02425.x.

806   Winkworth, R.E., 1973. Eco-physiology of Mulga (*Acacia aneura*). Tropical
807   Grasslands. 7: 43–48.

808   Wright, I.J., Falster, D.S., Pickup, M. and Westoby, M., 2006. Cross-species
809   patterns in the coordination between leaf and stem traits, and their implications for plant
810   hydraulics. Physiologia Plantarum. 127: 445–456, DOI: 10.1111/j.1399-
811   3054.2006.00699.x.

812   Zha, T.S., Li, C.Y., Kellomaki, S., Peltola, H., Wang, K.Y. and Zhang, Y.Q., 2013.
813   Controls of evapotranspiration and CO_2 fluxes from Scots pine by surface conductance
814   and abiotic factors. PLoS ONE. 8: e69027, DOI: 10.1371/journal.pone.0069027.

815   Zhang, Y.J., Meinzer, F.C., Hao, G.Y., Scholz, F.G., Bucci, S.J., Takahashi,
816   F.S.C., Villalobos-Vega, R., Giraldo, J.P., Cao, K.F., Hoffmann, W.A. and Goldstein, G.,
817   2009. Size-dependent mortality in a Neotropical savanna tree: the role of height-related
818   adjustments in hydraulic architecture and carbon allocation. Plant Cell Environ. 32: 1456–
819   1466, DOI: 10.1111/j.1365-3040.2009.02012.x.

820   Zhao, M.S. and Running, S.W., 2010. Drought-induced reduction in global
821   terrestrial net primary production from 2000 through 2009. Science. 329: 940–943, DOI:
822   10.1126/science.1192666.

823   Zolfaghar, S., Villalobos-Vega, R., Cleverly, J., Zeppel, M., Rumman, R. and
824   Eamus, D., 2014. The influence of depth-to-groundwater on structure and productivity of
825   *Eucalyptus* woodlands. Aust. J. Bot. 62: 428-437, DOI: 10.1071/BT14139.

826

827

828

829

8. Legends

831   Table 1. Summary of rainfall and net ecosystem productivity (NEP) for four years

832 of study at the Mulga woodland. Data for 2010–2012 from Eamus *et al*. (2013) and

833 Cleverly *et al.* (2013a).

834   Figure 1. Daily (a, b) and cumulative (c) precipitation in the Mulga woodland (a,

835 solid line c) and the *Corymbia* savanna (b, broken line c).

836   Figure 2. Daily (a) and cumulative (b) evapotranspiration (ET) in the Mulga

837 woodland (solid line) and the *Corymbia* savanna (broken line).

838   Figure 3. Daily (a) and cumulative annual (b) net ecosystem productivity (NEP) in

839 the Mulga woodland (solid line) and the *Corymbia* savanna (broken line). Daily values are

840 shown as the 3-day running average. Values of NEP that are larger than zero (dashed line)

841 represent carbon uptake.

842   Figure 4. Daily cycle of NEP. Values represent hourly average ± standard error

843 (s.e.) during January 2013.

844   Figure 5. Daily ecosystem water use efficiency (eWUE). Values were determined

845 as NEP/ET and shown for days when $ET > 0.2$ mm d^{-1}. Values above zero (dashed line)

846 represent photosynthetic eWUE, while increasingly negative values of eWUE represent

847 increasing values of respiratory eWUE.

848   Figure 6. MODIS enhanced vegetation index (EVI) as a four-month running

849 average.

850   Figure 7. Carbon stable isotope ratio ($\delta^{13}C$) of *Acacia* (squares) and *C. opaca*

851 (circles) leaves in the Mulga woodland and across three habitats (Mulga patch, open

852 savanna, transition) within the *Corymbia* savanna. Symbols show mean ± s.e.

853

854